Supplementary Material to the article "Delayed Photoluminescence Blinking of Single Semiconductor Quantum Dots: Novel Experiments and Modeling"

Note 1. Experimental setup

The experimental setup is based on home-build luminescent microscope-spectrometer with possibility to measure absolute and relative arrival times of photoluminescence (PL) photons in Hanbury Brown and Twiss scheme in time-tag mode at the pulsed excitation.

To excite the sample, we used a TOPOL (Avesta) femtosecond parametric oscillator with a wavelength of 580 nm, equipped with an electro-optical modulator to thin the pulse repetition rate to 1 MHz. This frequency made it possible to investigate the long-lived states of the system. The immersion microobjective CarlZeiss 100X, 1.3 numerical aperture (NA) was employed for focusing the laser beam and collecting the PL signal from single quantum dots (QDs). For registering the PL signal from single emitters, a high-sensitive cooling EMCCD-camera (Andor iXon Ultra) was used. The spectra were measured using an imaging astigmatism-corrected spectrometer (SOL Instruments).

In Hanbury Brown and Twiss scheme SPAD detectors (EG&G, SPCM-200PQ, QY ~ 60 % at 630 nm wavelength, "dark" time - 200 ns, time resolution - 1.3 ns) were used. The arrival times of photons and laser synchronization pulses were recorded using a multi-channel correlated photon counting (TCSPC) electronic scheme (Becker&Hickl DPC 230, time resolution ~165 ps).

Note 2. Calculation of time-gated PL traces

The principle of calculation PL and time-gated PL traces is schematically shown in Fig. S1. To plot the classic PL traces $I(t_i)$ (see top row of Fig. S1a), the total number of photons arrived between t_i and $t_i+\Delta t$ was counted. The resulting dependence $I(t_i)$ represents the temporal evolution of the total PL signal for a selected exposure time Δt. Time-gated PL traces (Fig. S1a, bottom row) were constructed the same way, but only photons delayed more than T_D relative to the excitation laser pulse were considered (time gate – [T_D, T], where T = 1 μs – laser repetition period).

Choosing the proper value of T_D allowed us to analyze the delayed PL separately from the whole signal. In this work T_D value was selected in the range from 100 to 200 ns. The choice of T_D was determined by the ratio of number of photons which come after T_D from delayed PL component to the total PL: $\int_{T_D}^{T} I_{delayed}(t)dt \,/\, \int_{T_D}^{T} I_{total}(t)dt$. This ratio determines the fraction of delayed PL in time-gated PL trace. Fig. S1b shows the fractions of prompt (black line) and delayed (red line) for different delays T_D calculated for the experimental data presented in Fig. 1 of the main text. At small delays prompt PL dominates in the signal, then around 140 ns the signal consists of the delayed component by more than 70 % and at big delays the main role is played by detector noise. To show the dynamics of delayed PL intensity on time-gated PL traces parameter T_D = 140 ns was chosen.

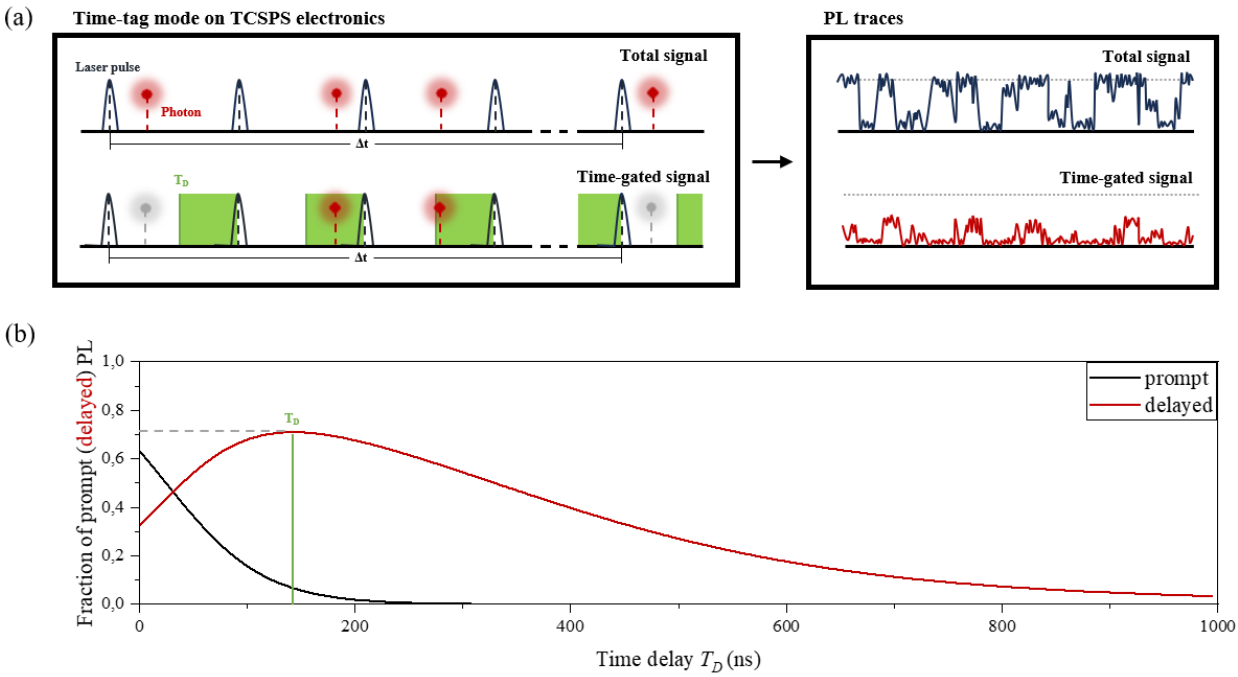

Fig. S1. (a) The principle of calculation PL (top row) and time-gated PL (bottom row) traces. In the calculation of time-gated traces, only photons arriving with a delay time greater than T_D are considered (red-colored). (b) Fraction of prompt (black) and delayed (red) PL components at time-gated PL trace for different delays T_D.

Note 3. Fast trapping influence on PL decay shape

Simulation results in Fig. S2 demonstrate the effect of the trapping rate k_t on the shape of the delayed PL decay curve considering the finite temporal resolution (~ 1.5 ns in our case). As one can see on the graph, the component corresponding to the fast trapping process disappears when trapping time $1/k_t$ is around 1 order of magnitude smaller than the time resolution.

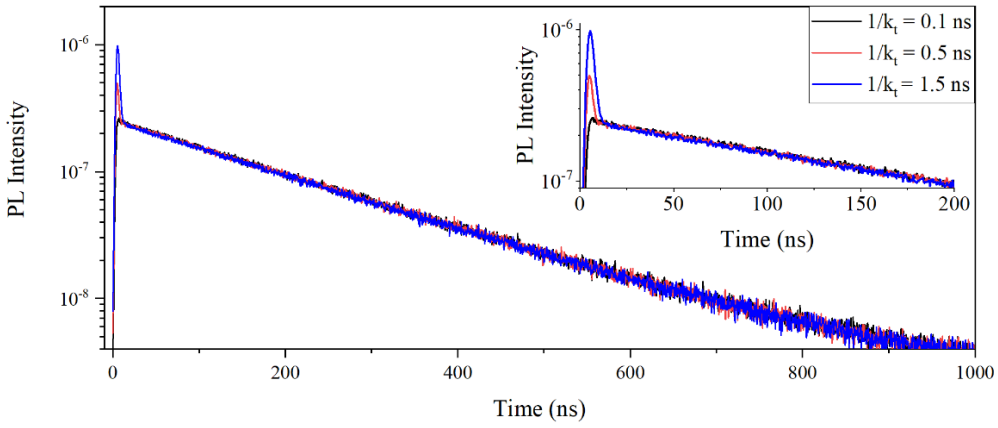

Fig. S2. Simulated decay curves of delayed PL at trapping time $1/k_t$ = 0.1, 0.5, and 1.5 ns. Time resolution is 1.5 ns.

Note 4. The key Monte Carlo simulation parameters

Table S1. The main fixed parameters used in the Monte Carlo simulation of delayed PL decay curves.

Time resolution, ns	Radiative time $1/k_r$, ns	Trapping time $1/k_t$, ns	NR recombination time from trap state $1/k_{NR}$, ns	Number of traps, N	Av. number of excitation per pulse	Excitation frequency, MHz
1.5	35	0.1	400	1	0.01	1

Note 5. Extended results of the Monte Carlo simulation

The extended simulation results are presented in Fig. S3. Panels (a) and (c) present decay curves (top) as well as lifetime and decay amplitude dependencies on the variable parameter (bottom) for Model 1 for cases of mono- and bi-exponential decays respectively. Panels (b) and (d) – for Model 2.

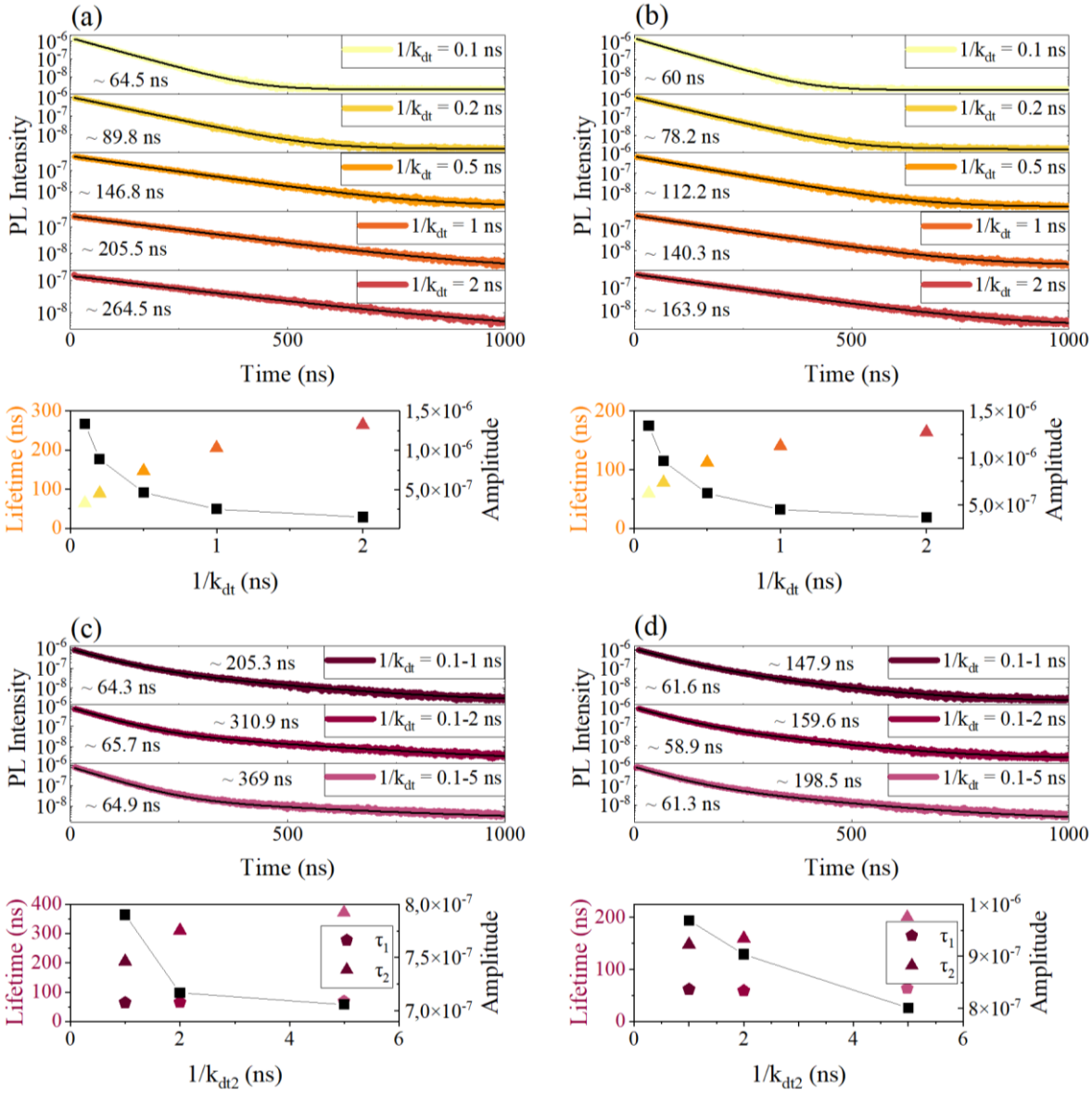

Fig. S3. Simulated decay curves of delayed PL for Model 1 (*a*, *c*) and Model 2 (*b*, *d*).

Note 6. Absence of delayed PL

Fig. S4 demonstrates experimental results for one of the investigated QDs, when delayed PL was not observed at all. PL decay (panel a) shows a pure mono-exponential dependence with an exciton lifetime τ = 34 ns. Time-gated PL traces for different delays T_D look almost identical and represent no signs of delayed PL activation.

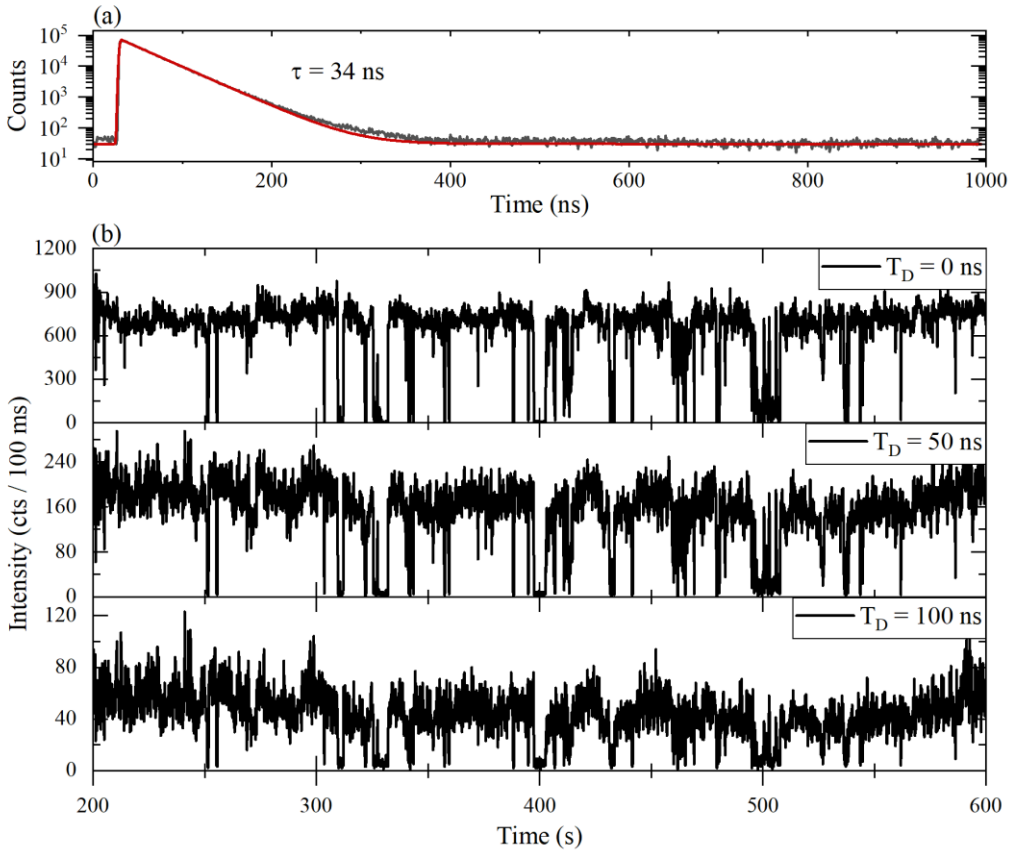

Fig. S4. Experimental results for one of investigated QDs without delayed PL. (a) PL decay curve. (b) stack with time-gated PL traces for delays T_D = 0, 50 and 100 ns.